Re-engineering 10-23 core DNA- and MNAzymes for applications at standard room temperature

Karen Ven[+], Saba Safdar[+], Annelies Dillen, Jeroen Lammertyn*, Dragana Spasic

Department of Biosystems, Biosensors Group, KU Leuven - University of Leuven, 3001, Leuven, Belgium
+Contributed equally to this work
**Corresponding author: jeroen.lammertyn@kuleuven.be • +3216321459 • orcid.org/0000-0001-8143-6794*

DNA- and MNAzymes are nucleic acid-based enzymes (NAzymes), which infiltrated the otherwise protein-rich field of enzymology three decades ago. The 10-23 core NAzymes are one of the most widely used and well-characterized NAzymes, but often require elevated working temperatures or additional complex modifications for implementation at standard room temperatures. Here, we present a generally applicable method, based on thermodynamic principles governing hybridization, to re-engineer the existing 10-23 core NAzymes for use at 23 °C. To establish this, we first assessed the activity of conventional NAzymes in the presence of cleavable and non-cleavable substrate at 23 °C as well as over a temperature gradient. These tests pointed towards a non-catalytic mechanism of signal generation at 23 °C, suggesting that conventional NAzymes are not suited for use at this temperature. Following this, several novel NAzyme-substrate complexes were re-engineered from the conventional ones, and screened for their performance at 23 °C. The complex with substrate and substrate-binding arms of the NAzymes shortened by four nucleotides on each terminus demonstrated efficient catalytic activity at 23 °C. This has been further validated over a dilution of enzymes or enzyme components, revealing their superior performance at 23 °C compared to the conventional 10-23 core NAzymes at their standard operating temperature of 55 °C. Finally, the proposed approach was applied to successfully re-engineer three other new MNAzymes for activity at 23 °C. As such, these re-engineered NAzymes present a remarkable addition to the field by further widening the diverse repertoire of NAzymes applications.

Keywords: DNAzyme, MNAzyme, room temperature, 10-23 core

INTRODUCTION

Enzymes are natural catalysts, essential for numerous life-sustaining processes, banking on their activity as oxidoreductases, transferases, isomerases, hydrolases, ligases, and lyases[1]. Whereas they are traditionally protein in nature, nucleic acid-based enzymes (NAzymes) have proven to be an important addition to the catalytic toolbox. For example, ribonucleic acid (RNA) enzymes (ribozymes) are naturally occurring catalytic molecules, providing support to the hypothesis of initial life arising from RNA[2]. Since their discovery three decades ago, numerous synthetic ribozymes have been selected using SELEX (systematic evolution of ligands by exponential enrichment) technology[3] and utilized thereafter for countless applications[4–6]. Alternatively, deoxyribonucleic acid enzymes (DNAzymes) have been developed as purely synthetic catalytic sequences without any natural counterparts[7]. However, both ribozymes and DNAzymes are made up of the same chemical building blocks and share the same flexibility in sequence design[8]. Moreover, they remain stable over a wide range of pH (3-10), temperature (4 °C - 63 °C), and buffer compositions[9–14], contrary to the protein enzymes, which require more stringent conditions for activity and storage. In this context, NAzymes are considered as promising catalytic alternatives in various applications.

DNAzymes catalyze an extensive repertoire of reactions, including peroxidation[15], Friedel-Crafts reaction[16], porphyrin metallation[17] and cleavage of RNA or RNA-DNA hybrid sequences[18]. The latter is performed by DNAzymes comprising of a catalytic core flanked by two substrate-binding arms. The arms hybridize with the substrate by virtue of Watson-Crick base pairing, resulting in cleavage by the catalytic core at the cleavage site with two RNA bases. There are two well-characterized classes of DNAzyme catalytic cores: the 8-17 and 10-23, named after the SELEX rounds each was discovered in[18]. Instances of their applications include metal sensing[19], molecular diagnostics[20, 21], and formation of nanodevices for sensing and *in vivo* monitoring[22, 23]. Additionally, the catalogue of applications has been further expanded by the DNAzyme-derived multicomponent nucleic acid enzymes (MNAzymes)[24–27]. MNAzymes are generated via division of the DNAzyme catalytic core into two halves and addition of an extra binding arm to each of them. The two resulting partzymes assemble in their catalytic form only in the presence of an oligonucleotide known as assembly facilitator (AF). Thus, the AF binds with the extra binding arms and enables cleavage of the substrate once it is bound to the substrate-binding arms of the partzymes. This MNAzyme design, which ensures assembly only in the presence of a trigger (target) sequence (i.e. AF), opened many more avenues for biosensing applications compared to the DNAzymes[28].

Although both DNA- and MNAzymes have been used in different biosensing and diagnostic applications, they mostly require elevated temperatures for their optimal functioning, implying that at least one step of the bioassay must occur at temperatures well above 23 °C[29–33]. So far, only the 8-17 core-derived NAzymes have been shown to function at room temperature without requiring initial heating steps or additional modifications[23, 34]. Efforts have been made to make 10-23 NAzymes compatible with lower temperatures. However, this was achieved so far only through complex physico-chemical modification of NAzymes (e.g. by introducing modified nucleotides or using cationic copolymers for reaction turnover enhancement[27, 35–38]), or by elevating temperature prior to the reaction[39, 40]. The latter more specifically poses issues when using NAzymes not only for DNA-target detection, but also for detection of other target molecules (e.g. small molecules or proteins), and when combining NAzymes with measurement setups that are not equipped with heating elements (e.g. microscopes and lateral flow tests, amongst others). Therefore, these temperature restrictions and/or complex modifications altogether precluded harnessing the full

potential of these broadly stable molecules and jeopardized their ease-of-use in biosensing applications.

In this context, here we present for the first time a very simple methodology to expand the functionality of existing 10-23 core DNA- and MNAzymes (collectively referred to as NAzymes in this paper) for use at 23 °C. The strategy relies solely on Watson-Crick base pairing and the thermodynamic principles governing hybridization, thus not requiring any complex physico-chemical modifications. To achieve this, we first studied the catalytic activity of conventional NAzymes at their optimal temperature of 55 °C as well as at our targeted temperature of 23 °C. Based on the generated novel insights of their behavior, we redesigned and screened different NAzymes and substrate sequences for their activity at 23 °C. Next, the most promising DNA- and MNAzymes complexes were further assessed over a range of concentrations. Finally, the generality of this approach to redesign NAzymes for application at 23 °C was evaluated by testing a second substrate sequence and, in addition, another AF sequence in order to redesign three completely novel 10-23 core MNAzymes. As such, these re-engineered 10-23 core NAzymes show great promise to considerably simplify bioassay development and implementation on different biosensing platforms.

MATERIALS AND METHODS

All NAzymes, substrates and the AF, summarized in Table S1, were purchased from IDT Technologies (Leuven, Belgium). Trident Tris.HCl (1 M, pH 8.8, Genetex Inc., Irvine, USA), potassium chloride (KCl, 99%+, Acros Organics, Geel, Belgium) and magnesium chloride solution ($MgCl_2$, 1 M, Fisher Scientific, Leicestershire, England) were used without further purification. All solutions were prepared using UltraPure distilled water (DNAse-RNAse free, Invitrogen, Carlsbad, USA). Tris-Ethylenediaminetetraacetic acid (TE, 100 X, Sigma-Aldrich, St. Louis, USA) buffer solution was used for preparation of the working solutions of the oligonucleotides, unless otherwise indicated. All reaction mixes were prepared in DNA-LoBind tubes (1.5 mL, Eppendorf, Hamburg, Germany) and the fluorescence was measured in 384–well clearbottom microplates (Glasatelier Saillart, Meerhout, Belgium) or PCR tubes (Qiagen, Hilden, Germany).

Design of NAzymes and substrates. The $DNAzyme_{long}$ (nr 1 in Table S1, Electronic Supplementary Material), the $MNAzyme_{long}$ (comprising of partzyme A_{long}, partzyme B_{long} and the corresponding AF sequence (nr 4, 9 and 15 in Table S1, respectively)) and the substrate (nr 17 in Table S1) are adapted from previously published sequences[41] to preclude the need of a high-temperature denaturation step. The short NAzymes (nr 3, 5 and 11 in Table S1) were re-engineered by shortening the substrate-binding arms with four bases on each terminus. The short substrate was edited accordingly to match the length of the substrate-binding arms of the NAzymes (nr 20 in Table S1). All cleavable substrates are DNA in nature, but contain two RNA bases at the cleavage site. A non-cleavable substrate was engineered by replacing these two RNA bases with their DNA counterparts (nr 19 in Table S1). All substrates were labelled on the 5' end with a fluorescent FAM label and on the 3' end with Iowa Black FQ (IBFQ) quencher molecule, with exception of the substrate that was internally labelled with FAM (nr 18, Table S1). To enable this internal labelling, adenine in the substrate was substituted with a thymidine base (highlighted in grey in Table S1), acting as a tether for the internal FAM label, whereas the complementary base in the substrate-binding arm of the NAzymes was altered accordingly (nr 2 and 10 in Table S1). The melting temperatures and secondary structures of these sequences were analyzed using the OligoAnalyzer 3.1 tool of IDT Technologies (https://eu.idtdna.com/calc/analyzer). The Tm of the intact substrate was calculated by approximating a standard duplex, formed between the substrate strand with 2 RNA bases and its DNA complement. The Tm of the 3' half of the substrate was calculated as the Tm of a standard duplex, starting with the RNA-U base (in the substrate strand) and A base in the complementary strand, as the latter is also incorporated in the complementary substrate-binding arm of the NAzyme. The Tm of the 5' half of the substrate was calculated as the Tm of a standard duplex while excluding the RNA-G base, since its complement is not incorporated in the corresponding substrate-binding arm of the NAzyme. The theoretical method of assessing the melting temperatures was preferred over the experimental method, considering the temperature-mediated degradation of the substrate at temperatures above 75 °C, due to the presence of RNA bases (Figure S1, Electronic Supplementary Material).

Assessment of NAzyme activity. The activity of the NAzymes was evaluated in 25 µL of the reaction mix, containing 250 nM of DNAzyme or 250 nM of each of the partzymes and the AF, and 250 nM of the appropriate substrate. All reactions were prepared in 10 mM Tris-HCl with 50 mM KCl, and 20 mM $MgCl_2$ (pH 8.3). All dilutions were prepared from 10 µM stock solutions in TE and all reagents were kept on ice until the final readout. The activity of the conventional NAzymes was measured at 55 °C and over temperatures ranging from 75 °C to 35 °C and back to 75 °C, with steps of 10 °C, using the Rotor-Gene Q real-time PCR cycler (Qiagen, Venlo, Netherlands). Fluorescence was measured every 30 seconds for 5 minutes at each step via signal acquisition through the green channel. The NAzyme activity at 23 °C was monitored kinetically on a SpectraMax M-series microplate reader (Molecular Devices LLC, San Jose, USA) with excitation at 485 nm and emission at 583 nm, measuring fluorescence every minute for 30 minutes. To evaluate the performance of the NAzymes, the signal-to-noise ratio (SNR) was calculated as the ratio of the fluorescent signal generated by the functional NAzyme and the fluorescent signal of the substrate itself. All measurements were performed in triplicates. The different controls and test reactions performed are depicted in **Figure 1**.

Characterization of redesigned NAzymes. The concentration-dependent activity of the NAzymes was tested with a 5-fold dilution (250 nM, 50 nM, 10 nM) of NAzymes with 250 nM of substrate, in a total volume of 25 µL. As a negative control, we included a sample without NAzymes (0 nM). In addition, the MNAzyme activity was evaluated over a 5-fold dilution of the AF,

with the partzymes and substrate kept at fixed concentration of 250 nM. All measurements were performed in triplicate. The measurements at 23 °C were acquired using a SpectraMax M-series microplate reader and the 55 °C measurements were obtained using a Rotor-Gene Q real-time PCR cycler, as detailed in the previous section. To account for the difference in fluorescence readings between both devices and enable comparison of the results, the SNR was calculated as explained above.

Validation of redesigning approach. The validity of the approach to redesign NAzymes was evaluated by starting from another previously published substrate sequence[28] and shortening it by 9 nucleotides (nr 21 in Table S1), resulting in a sequence of the same length as the previously shortened substrate. This substrate sequence was labeled with a fluorophore and quencher as described above. Moreover, a novel AF was implemented, representing a fragment of the genomic sequence of *Streptococcus pneumonia* (nr 16 in Table S1). Using these elements, 3 novel short MNAzymes were generated with the sequences of all partzymes listed in Table S1 (nr 6 - 8 and 12 - 14). The performance of these newly redesigned MNAzymes was evaluated in 25 µL of the reaction mix, containing 250 nM of each of the partzymes and the AF, and 250 nM of the appropriate substrate. Reaction mixtures were prepared as detailed above. Readout was performed at 23 °C in the microplate reader, using the previously described settings. All measurements were performed in triplicates.

RESULTS AND DISCUSSION

Performance of conventional NAzymes at 55 °C and 23 °C. First, we examined the performance of the conventional NAzymes (DNAzyme sequence nr 1 and MNAzyme sequences nr 4 and 9 in Table S1) at the recommended working temperature of 55 °C[41]. To do that, we used a cleavable substrate, terminally labelled with a fluorophore and quencher molecule. The latter effectively decreases the fluorescence intensity of the fluorophore (Förster Radius of 57.9 Å) when the substrate is in its intact conformation.

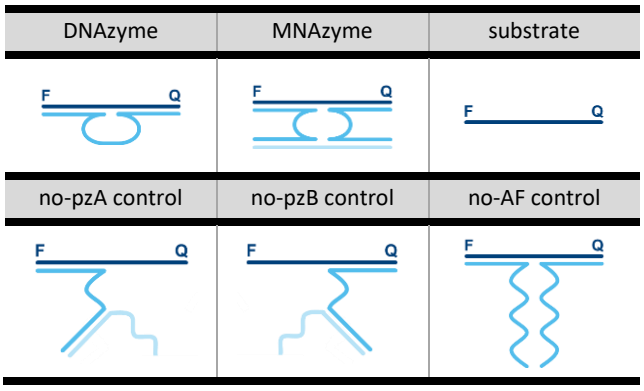

Figure 1 Schematic representation of different test reactions and controls, including the functional DNAzyme, functional MNAzyme, substrate background, and the controls for the MNAzyme when omitting the AF (no-AF), partzyme A (no-pzA) or partzyme B (no-pzB).

Consequently, incubation of both NAzymes with fluorogenic substrate resulted in fluorescence increase, suggesting successful cleavage of the substrate and separation of the quencher and fluorophore (Figure 2). In the absence of the AF (no-AF control, **Figure 1**), the active MNAzyme complex was not formed and the substrate was not cleaved, as reflected with the marginally increasing fluorescent signal. Similarly, lack of either of the two partzymes (no-pzA and no-pzB control, **Figure 1**) resulted in a fluorescent signal not distinguishable from the background signal of the substrate, confirming that the incomplete MNAzyme is unable to cleave the substrate. It should be noted that, whereas the NAzymes were kept on ice prior to the readout, they became catalytically active while the device was reaching the measurement temperature of 55 °C, resulting in an initial offset fluorescence for both the DNA- and MNAzyme.

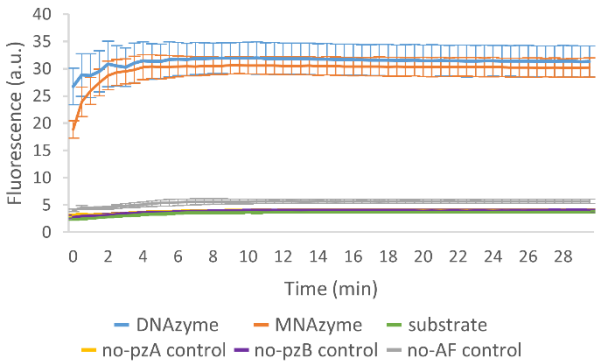

Figure 2 Performance of the conventional NAzymes at 55 °C in the presence of the cleavable substrate. The signal of the functional DNAzyme and MNAzyme is displayed, in addition to the substrate background and the controls of the MNAzyme in the absence of the AF, partzyme A or partzyme B. The signal from the functional NAzymes was clearly distinguishable from the controls, indicating successful substrate cleavage at an operating temperature of 55°C. All components were present in a concentration of 250 nM. The error bars represent the standard deviation of 3 independent repetitions, measured with a real-time PCR cycler.

Next, we assessed the activity of these conventional NAzymes at 23 °C, as depicted in Figure 3a. Although the fluorescent signal obtained when using the functional DNAzyme and MNAzyme was significantly higher than the substrate background, it partially overlapped with the no-AF, no-pzA and no-pzB control signals. Because these controls represent inactive NAzyme complexes, the observed fluorescence at 23 °C suggested the presence of an effect other than cleavage of the substrate. To test this hypothesis, the same assay was performed with a substrate which could not be cleaved and thus not lead to an increased fluorescence over time (Figure 3b). This non-cleavable substrate was engineered by replacing the two RNA bases that form the cleavage site of the NAzymes with two DNA bases. As shown in the figure, the fluorescent signal generated by the functional NAzymes was significantly higher compared to the substrate background, even when incubated with non-cleavable substrate. Moreover, these signals were comparable to the control signals of the incomplete and thus inactive MNAzymes (no-AF, no-pzA and no-pzB control) as well as to the NAzymes signal in the presence of the cleavable substrate (Figure 3a). These results pointed towards a cleavage-independent increase in fluorescence at 23 °C, hampering the use of conventional NAzymes under these conditions.

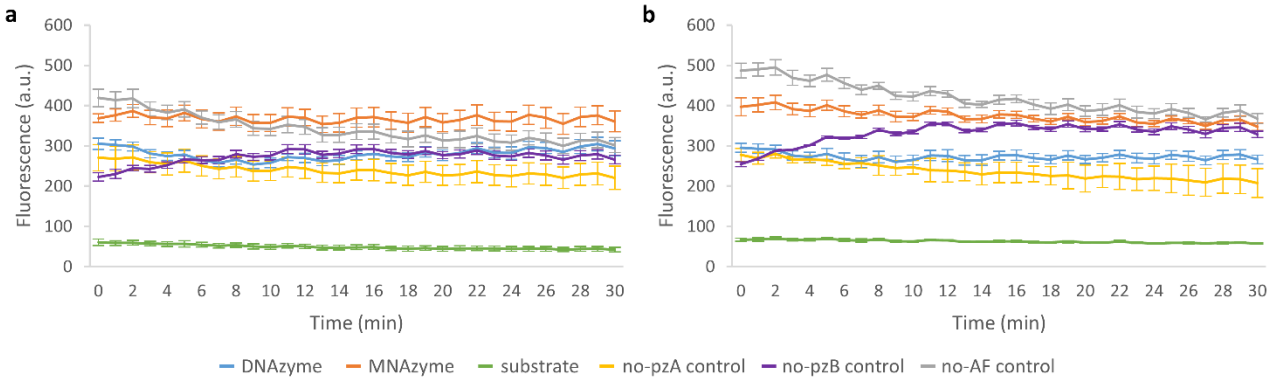

Figure 3 Performance of the conventional NAzymes at 23 °C in the presence of A. the cleavable substrate, demonstrating that the functional NAzymes cannot be used at this temperature due to the overlapping fluorescent signals with the control signals (i.e. incomplete NAzymes) and B. the non-cleavable substrate, revealing that the observed increase in fluorescence for the functional NAzymes and the controls, when compared to the substrate background, was not arising from enzymatic cleavage. The signal of the functional DNAzyme and MNAzyme is depicted, as well as all controls, including the substrate background and the controls of the MNAzyme in the absence of the AF, partzyme A or partzyme B. All components were present in a concentration of 250 nM. The error bars represent the standard deviation of 3 independent repetitions, measured with a microplate reader.

Energetic considerations of conventional NAzymes. In order to decipher the origin of the observed fluorescent signals at 23 °C, we estimated the melting temperatures (Tm) of the utilized sequences using the OligoAnalyzer tool. As shown in Table 1, we first estimated the Tm of the intact conventional substrate sequence (Sub_{long}), which corresponds to the Tm of the entire complex formed by hybridization of both substrate-binding arms of the NAzymes to the complete substrate. Next, we also estimated the Tm of the 2 halves of the substrate, generated after cleaving: (1) the 3' half, which is complementary to the substrate-binding arm of both the 5' end of the DNAzyme and partzyme A, and (2) the 5' halve, which is complementary to the substrate-binding arm of both the 3' end of the DNAzyme and partzyme B. It should be noted that for the latter, the guanine RNA-base is excluded as it is not complementary to either of the substrate-binding arms of the NAzymes.

In the studies conducted at 55 and 23 °C, both working temperatures were below the calculated Tm of the complete Sub_{long} sequence and thus of the completely hybridized complex (68.1 °C), enabling hybridization of the NAzymes to the substrate and its cleaving. Moreover, at 55 °C, the cleaved substrate strands could dissociate from the individual substrate-binding arms since the working temperature was above their Tm values (43.9 and 44.6 °C). In contrary, the experiments at 23 °C were performed well below the Tm of the cleaved substrate strands, preventing them to dissociate from the NAzymes after cleavage and thus impairing signal generation. Despite this, an increase in fluorescent signal was still observed (Figure 3a), suggesting that other events were taking place at 23 °C. Here we hypothesize that the substrate, once hybridized to the substrate-binding arms of the NAzyme, changes in conformation from a compact, single-stranded structure to a more elongated double-stranded structure. As a result of this stretching of the substrate, the fluorophore would be moved further away from the quencher. This in turn would decrease the effect of the quenching molecule and thus partially increase the fluorescence of the substrate molecules without releasing the cleaved substrate strands. This theory was further supported by the comparable fluorescent signal obtained when both cleavable and non-cleavable substrates were used at 23 °C (Figure 3). Since the latter could not be cleaved, the apparent signal had to be cleavage-unrelated.

Table 1 Estimated Tm of the intact and cleaved sequences of the conventional, long (Sub_{long}) and short (Sub_{short}) substrate. The 3' half represents the part of the substrate that is complementary to the substrate-binding arm of partzyme A. The 5' half of the substrate represents the part of the substrate that is complementary to the substrate-binding arm of partzyme B. These estimations are based on a salt concentration of 50 mM monovalent and 20 mM divalent ions, and a DNA concentration of 250 nM.

T_m	Sub_{long}	Sub_{short}
intact substrate	68.4 °C	54.4 °C
3' half of the substrate	43.9 °C	8.1 °C
5' half of the substrate	44.6 °C	9.6 °C

The results obtained for the MNAzyme-controls (no-AF, no-pzA and no-pzB control) were also in line with this hypothesis. Here, the unimolecular-like structure could not be formed in the absence of any of the three components, precluding effective availability of the substrate-binding arms. Therefore, at 55 °C, the individual arms did not hybridize to the substrate as the working temperature was almost 10 °C above their Tm. This was illustrated by the low fluorescent signal obtained for the control samples at 55 °C (Figure 2). At 23 °C, however, the individual substrate-binding arms could hybridize to the substrate, even in the absence of the facilitator, as the Tm was not trespassed. Therefore, hybridization-related stretching of the substrate occurred without actual cleavage, contributing to the observed increase in fluorescence for the control samples (Figure 3).

To gain further insight into the observed mechanisms at 23 °C, we monitored the NAzyme-mediated generation of fluorescent signal while decreasing the temperature from 75 to 35 °C and

subsequently increasing it back to 75 °C in steps of 10 °C, each lasting for 5 minutes (Figure 4). It should be noted that, due to limitations of the qPCR setup, the minimal temperature was 35 °C instead of 23 °C, used in the previous experiments with the microplate reader. Nevertheless, even 35 °C is well below the Tm values of individual substrate-binding arms (43.9 and 44.6 for Sub_{long} sequence, Table 1), suggesting that similar mechanisms will take place at this temperature as they would at 23 °C.

Overall, a stepwise increase in signal was observed with decreasing temperature, followed by a stepwise signal decrease upon the subsequent increase in temperature. The latter can be explained in part by the fact that the fluorescence intensity of a fluorophore decreases[42] whereas the efficacy of a quencher increases[43] with increasing temperature. Note that this trend is not present for the substrate control (i.e. in the absence of the enzyme), as the quencher molecules are present in close proximity to the fluorophores in the intact substrate. In addition to temperature effects, the signal profile suggested involvement of other, complex phenomena as well, as illustrated by the following findings: (1) the fluorescence profile of the functional MNAzymes varied from that of the functional DNAzyme when decreasing the temperature from 75 °C to 35 °C and (2) after re-increasing the temperature, the fluorescence did not return to the baseline level for the functional NAzymes while it did for the controls. The first finding can be explained by the slightly more stable hybridization of the DNAzyme with its substrate, compared to the MNAzyme, because of its true unimolecular nature. This enabled the DNAzyme to cleave (a) at a higher rate (in agreement with previously published results[28]), as revealed by a significantly higher initial offset fluorescence, and (b) in more stringent conditions, as the maximal increase in fluorescence and a small kinetic trace appeared at a higher temperature for the DNAzyme (65 °C) than for the MNAzyme (55 °C). Nevertheless, both NAzymes reached comparable signals at 55 °C and followed a similar trend from there on, although never returning back to the initial fluorescence value. This illustrates once more that the signal of the functional NAzymes was largely generated through substrate cleavage, a process which could not be reversed by re-increasing the temperature. The latter was in sharp contrast with the fluorescence of the control samples, which was fully reversible, implying to be caused by non-cleavage associated mechanisms such as stretching of the substrate. It is important to note that at low temperatures (i.e. 45 and 35 °C), the signal of the no-AF control was approximately twice as high as the signal of the no-pzA and no-pzB controls. This illustrated that the signal of the substrate, when stretched by both partzymes, can be approximated by the summation of the stretching-induced signal of the individual partzymes. Since the no-AF control thus reflects the maximal level of stretching that can potentially occur, the no-pzA and no-pzB controls were omitted from the following experiments. Moreover, these experiments suggested that non-cleavage associated generation of a fluorescent signal due to substrate stretching occurs not only at 23 °C, as observed previously in the a microplate reader (Figure 3), but as well at all the other temperatures below the Tm values of the individual substrate-binding arms.

Together, these data revealed two restrictions that have to be addressed when working with conventional NAzymes at room temperature: (1) hybridization-induced stretching of the substrate results in increased control signals, which negatively impacts the sensitivity of the assay and (2) the high Tm of the cleaved substrate strands prevents it from dissociating from the NAzyme at 23 °C, thereby impeding signal generation and amplification.

Performance of redesigned NAzymes at 23 °C. To address the issues pertaining to the activity of NAzymes at room temperature, we redesigned the conventional NAzyme and substrate sequences and assessed their performance at 23 °C (Figure 5).

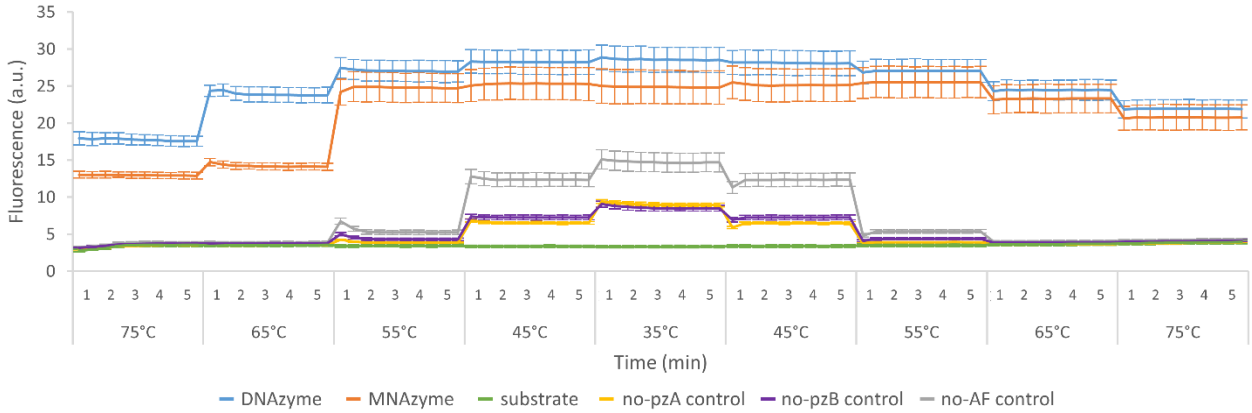

Figure 4 Performance of the conventional NAzymes at different temperatures, ranging from 75 °C – 35 °C – 75 °C with incremental steps of 10 °C, each lasting for 5 min. The signal of the functional DNAzyme and MNAzyme is displayed, in addition to the substrate background and the controls of the MNAzyme in the absence of the AF, partzyme A or partzyme B. The reversibility of the fluorescent signals for controls indicated a strong, temperature-dependent stretching effect of the substrate. Contrary to that, the fluorescent signal obtained with the functional NAzymes did not return to the baseline level, indicating that part of the observed signal is due to irreversible cleavage of the substrate by the functional NAzymes. The DNAzyme showed its catalytic activity under more stringent conditions than the MNAzyme, as demonstrated by the maximal increase in fluorescence and small kinetic trace at 65 °C and 55 °C for the DNA- and MNAzyme, respectively. All components were present in a concentration of 250 nM. The error bars represent the standard deviation of 3 independent repetitions, measured with a real-time PCR cycler.

Since hybridization to the substrate was found to be crucial in this context, we explored two substrate-related modification strategies without altering the NAzyme catalytic core or facilitator-binding arms: (1) labelling of the substrate sequence with the fluorophore internally (rather than terminally as in the previous experiments), to bring the fluorescent molecule closer to the quencher (nr 18 in Table S1) and (2) shortening the terminally-labelled substrate sequence with eight bases by removing four bases at each terminus (nr 20 in Table S1). The latter not only enabled to decrease the distance between the fluorophore and quencher, but also decreased the T_m of the cleaved substrate strands (Sub_{short}, Table 1), enabling them to dissociate from the NAzymes more easily at 23 °C. Similarly, the NAzymes were altered by shortening both substrate-binding arms, without modifying the AF-binding arms of the MNAzyme (nr 5 and 11 in Table S1). Combination of the redesigned substrate sequences and substrate-binding arms resulted in the generation of four new complexes (Complexes II – V, Figure 5a), in addition to the original Complex with the conventional NAzymes (Complex I).

The fluorescent signals of the screened complexes, as well as the SNR of the DNAzymes and MNAzymes, are depicted in Figure 5b. When compared to the conventional NAzymes (Complex I), the combination of the full-length NAzymes with the internally labelled substrate (Complex II) showed an increased signal for the functional DNAzyme and a reduced signal for the no-AF control. The latter suggested that reducing the distance between the fluorophore and quencher can indeed decrease stretching-induced fluorescence, although not improve the NAzyme activity. Alternatively, combining the full-length substrate with the shortened NAzymes (Complex III) induced a substantial drop in the signal of both the functional DNA- and MNAzyme, with the latter differing only marginally from the no-AF control. This could be attributed to the full-length substrate being more stable in solution than bound to the short substrate-binding arms of the NAzymes, thus hampering substrate hybridization, cleavage or stretching.

On the contrary, when using shortened substrate strands with either the full-length or shortened NAzymes (Complex IV and V, respectively), the obtained signal and SNR was substantially higher than any other tested complex, including conventional Complex I. Moreover, no-AF controls were significantly lower than the conventional complex, indicating a reduction of the stretching-induced portion of the signal. Whereas both complexes demonstrated the great benefit of shortening the substrate, it was decided to continue with Complex V due to the overall higher fluorescence intensity and SNR. This difference in performance with Complex IV could be explained by the repulsive effect of the negatively charged, overhanging parts of the substrate-binding arms, potentially hampering substrate hybridization and cleaving to a limited extent.

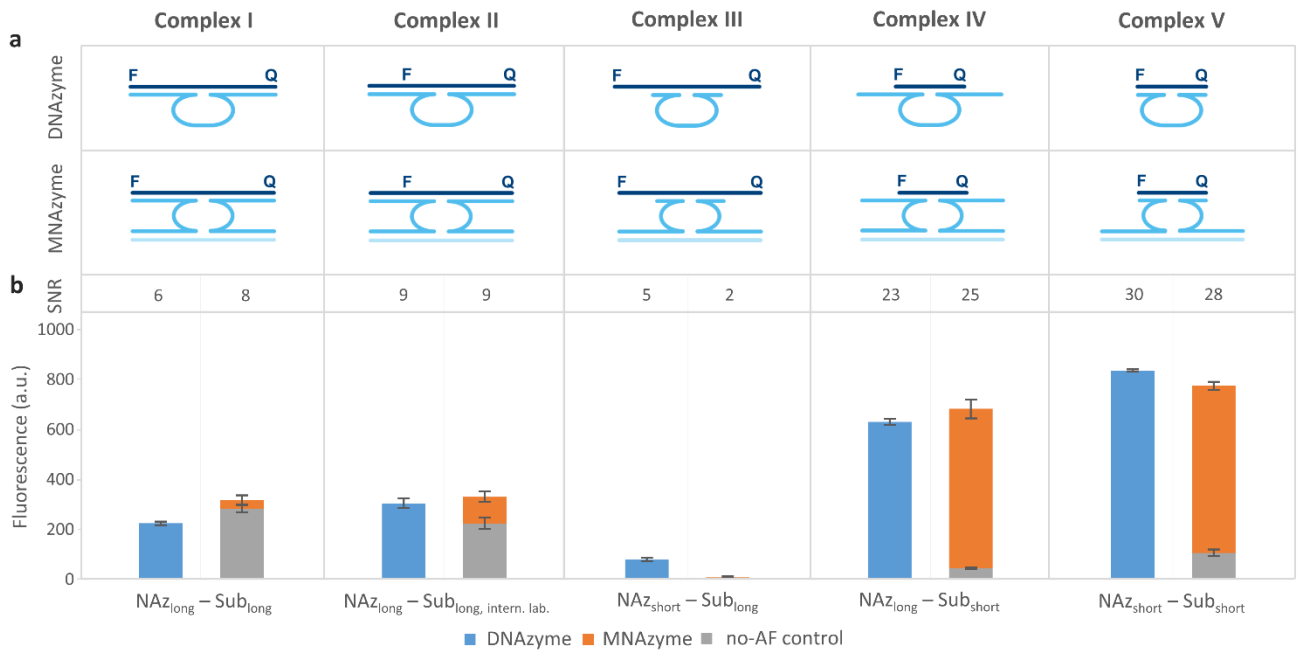

Figure 5 Performance of various NAzyme (NAz) and substrate (Sub) complexes at 23 °C. A. Schematic representation of the conventional NAzymes (Complex I) and the redesigned NAzymes, including: the conventional NAzymes in combination with the full-length, internally-labeled substrate (Complex II), the NAzymes with shortened substrate-binding arms in combination with the full-length substrate (Complex III), the conventional NAzymes in combination with the shortened substrate (Complex IV) and the NAzymes with shortened substrate-binding arms in combination with the shortened substrate (Complex V). B. Fluorescence readout of the conventional and redesigned NAzymes after 15 minutes. For each complex, the signal of the functional DNAzyme, the functional MNAzyme and, for the latter, the no-AF control is displayed. Amongst the five evaluated complexes, only Complex IV and V enabled clear discrimination between the functional MNAzyme and the no-AF control at 23 °C, with Complex V overall demonstrating the highest SNR. All components were present in a concentration of 250 nM and readout was performed in a microplate reader. The error bars represent the standard deviation of 3 independent repetitions after normalization for the substrate background.

Nevertheless, it should be noted that, depending on the type of application of the NAzymes at 23 °C, one could consider to use the full-length MNAzyme combined with the short substrate (Complex IV), since it did demonstrate a lower control signal in the absence of the facilitator (Figure 5).

Further characterization of redesigned NAzymes. Next, we evaluated the performance of Complex V at 23 °C by testing decreasing concentrations (50 and 10 nM) of the NAzymes with a fixed substrate concentration of 250 nM (Figure 6a). Note that the results of the 250 nM condition are included here as a reference (i.e. a single turnover reactions) whereas the enzyme dilutions represent multiple turnover conditions. As a negative control, we also included a sample without NAzymes (0 nM). The obtained fluorescent signals showed a clear concentration-dependency, which is a promising feature for the application of the redesigned DNA- and MNAzymes at 23 °C. As opposed to the previous reports on the implementation of NAzymes at room temperature[32, 35, 36, 38, 44], here there was no need for additional complex modifications or elevated temperatures to initiate the reaction. Although out of the scope of this research, additional experiments could be performed in the multiple turnover regime to gain further insight in the enzymatic rate of the redesigned NAzymes.

In addition, the performance of the redesigned DNA- and MNAzymes was compared to the performance of the conventional sequences (Complex I) at their recommended working temperature (55 °C). Whereas the latter also demonstrated a clear concentration-dependent fluorescent signal (Figure 6b), true comparison of both complexes required calculation of their SNRs. Interestingly, both the redesigned DNA- and MNAzyme performed better at 23 °C than the conventional ones at 55 °C, as indicated by the higher SNR. Moreover, the redesigned MNAzyme truly outperformed the conventional MNAzyme at their respective temperatures, as the signal obtained when using 10 nM of conventional NAzyme at 55 °C could not be reliably discriminated from the substrate background. It is important to note that obtaining a complex that works at 23 °C brings another advantage because of the intrinsically higher fluorescence levels at lower temperatures[42], as demonstrated by the overall improved SNR at 23 °C.

To further evaluate the performance of redesigned MNAzymes at 23 °C, we tested different concentrations of AF (250, 50 and 10 nM), while keeping the MNAzyme and substrate concentration constant (250 nM). This is important for the potential use of MNAzymes in a sensor, especially when the AF represents a nucleic acid target[28]. Similar to previous experiments, a control with 0 nM of the AF was included as well.
The obtained fluorescent signals (Figure 7a) revealed a clear concentration-dependency (irrespective of the turnover conditions), demonstrating the potential of implementing the redesigned MNAzymes in a sensor for target detection at 23 °C. Furthermore, when the SNR of the conventional MNAzymes at 55 °C (Figure 7b) was compared to that of the redesigned MNAzymes, the latter performed comparable if not slightly better (even though the assay conditions were not profoundly optimized), revealing their huge potential for implementation in various applications at room temperature.

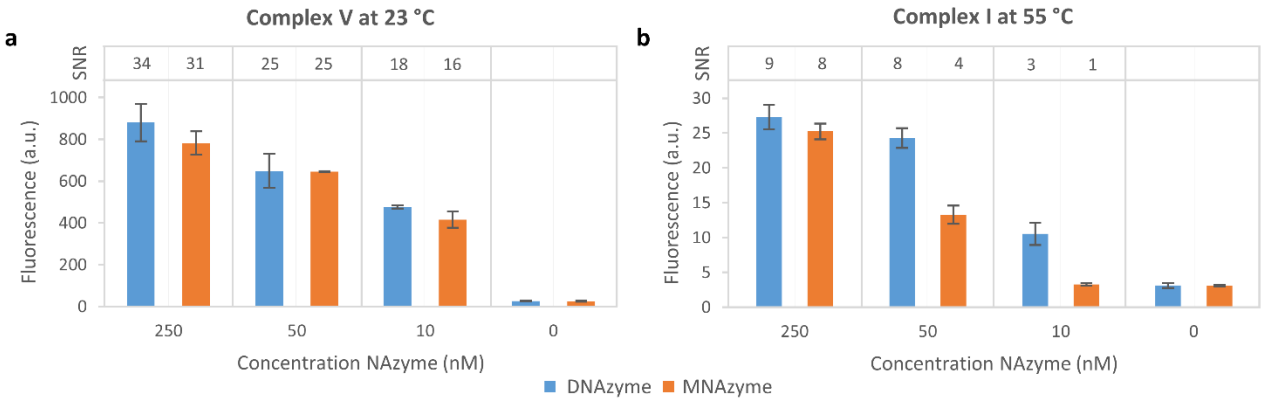

Figure 6 Performance of A. the redesigned (Complex V) and B. conventional (Complex I) NAzymes at their respective working temperatures, measured in a microplate reader and real-time PCR cycler, respectively. A 5-fold dilution series of the redesigned DNA- and MNAzyme molecules was tested, ranging from 250 to 10 nM with a constant substrate concentration (250 nM). 0 nM represents the control without NAzymes. The re-designed Complex V showed a much higher SNR at 23 °C when compared with the SNR of the conventional Complex I at its recommended temperature of 55 °C. The error bars represent the standard deviation of 3 independent repetitions.

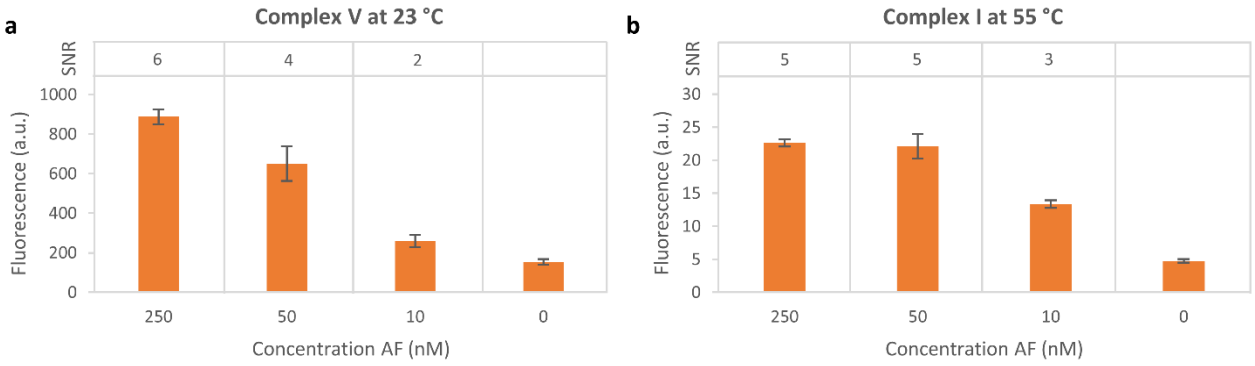

Figure 7 Performance of A. the redesigned (Complex V) and B. conventional (Complex I) MNAzymes at their respective working temperatures and measured in a microplate reader and real-time PCR cycler, respectively. A dilution series of the AF was evaluated, ranging from 250 nM to 10 nM for a constant concentration of redesigned MNAzyme and substrate (250 nM). A control with 0 nM AF was included. The redesigned MNAzyme (Complex V) demonstrated a concentration-dependent signal over the tested range of AF, signifying the potential of using this complex for a multitude of applications at room temperature. The error bars represent the standard deviation of 3 independent repetitions.

Validation of redesigning approach. Finally, we evaluated the general applicability of our approach to redesign 10-23 core MNAzymes for application at 23 °C. To do so, we generated three new MNAzymes, based on the previously redesigned MNAzyme of Complex V (referred to as MNAzyme 1 in **Figure 8**a): (a) MNAzyme 2, with a new substrate sequence, adapted from a previously reported one for use at 55 °C[28], by shortening it in the same manner as described above and adjusting the substrate-binding arms of MNAzyme 1 accordingly, (b) MNAzyme 3, with a new AF sequence and AF-binding arms while preserving the rest of MNAzyme 1, and (c) MNAzyme 4, with a combination of the novel AF and substrate sequences while conserving the catalytic core of MNAzyme 1. As can be seen from the fluorescence intensity and SNR in **Figure 8**b, these novel, redesigned MNAzymes performed equally well at 23 °C as the originally redesigned MNAzyme. As such, these results demonstrated the generality and simplicity of our approach to redesign MNAzymes for implementation at 23 °C, making it of high interest for a large number of applications.

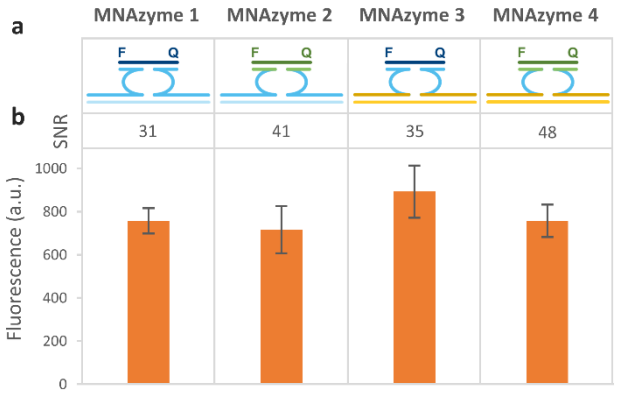

Figure 8 Performance of novel, redesigned MNAzymes at 23 °C. A. Schematic representation of the three newly redesigned MNAzymes, including the initially redesigned MNAzyme of Complex V (MNAzyme 1), the MNAzyme with an altered substrate sequence (MNAzyme 2), an altered AF sequence (MNAzyme 3) and a combination of altered substrate and AF into a new 10-23 core MNAzyme (MNAzyme 4). B. The fluorescent signal and SNR of the newly redesigned, functional MNAzymes. The overlapping fluorescent signals indicated that the methodology of re-designing NAzymes is generally applicable to other sequences, further demonstrating the flexibility and robustness of the system. Fluorescence readout was performed in a microplate reader after 15 minutes. All components were present in a concentration of 250 nM. The error bars represent the standard deviation of 3 independent repetitions after normalization for the substrate background.

CONCLUSIONS

NAzymes have recently emerged as promising DNA-based alternatives for the less stable and more sensitive protein-based enzymes. Whereas the 10-23 core NAzymes are well characterized and implemented in a variety of applications, they often require elevated working temperatures (> 25 °C) or initial heating steps. Consequently, limited examples can be found with these NAzymes working at room temperature, only upon complex chemical modification of their sequences or additional immobilization strategies. To expand their potential, we present in this work a generally applicable approach for redesigning existing 10-23 core NAzymes sequences, specifically for performance at 23 °C. First, we demonstrated the inadequate performance of conventional 10-23 core NAzymes at 23 °C. This was done by (1) comparing their activity in the presence of a cleavable substrate as well as a non-cleavable substrate at 23 °C and (2) monitoring the NAzyme activity over a wide range of temperatures (35 – 75 °C). Both approaches revealed a substantial background signal being generated either in the presence of cleavable substrates or incomplete (and thus not functional) MNAzymes, suggesting that hybridization-related substrate stretching mechanisms were taking place rather than enzymatic cleaving of the substrate. Based on this knowledge, we re-engineered conventional NAzyme and substrate sequences by altering their thermodynamic properties and decreasing the potential substrate stretching distance. We screened four novel complexes for their specific catalytic activity at 23 °C, finding two with an improved catalytic performance (i.e. SNR) at this temperature. Of these two complexes, comprising of shortened substrate and conventional or shortened substrate-binding arms, the complex with matching length of the substrate-binding arms and the substrate (so called Complex V) revealed an overall superior performance. Therefore,

it was further tested at 23 °C for its ability to generate concentration-dependent fluorescent signals. Under these conditions, re-engineered NAzymes were found to outperform the conventional ones at their recommended temperature (55 °C). In addition, we also tested the ability of the redesigned MNAzymes to discriminate various AF concentrations (down to 10 nM) at 23 °C, observing similar performance compared to the conventional counterparts and demonstrating their potential for implementation in a biosensor. Next, the universality of our approach was demonstrated by assessing the performance of three new MNAzymes, generated by redesigning the substrate sequence, AF sequence or both sequences when compared to Complex V. All three proved to perform equally well as the initially redesigned MNAzyme at 23 °C.

As such, this study reports an approach to successfully redesign well-known 10-23 core NAzyme sequences for their application at room temperature, precluding the need for additional nucleotide modifications or thermal triggers. This enables to (1) simplify platforms and bioassays, which is extremely valuable when using NAzymes for diagnostics applications; (2) prevent denaturation/degradation of non-nucleic acid targets at high temperatures when using NAzymes for detection of small molecules or proteins and (3) facilitate the implementation of NAzymes on measurement systems that do not enable heating. Whereas further research is required to elucidate the kinetic principles of these re-engineered NAzymes, their outstanding performance at room temperature demonstrates their huge potential in a wide variety of applications, including biosensing.

CONFLICTS OF INTEREST

The authors declare that they have no conflict of interest.

ACKNOWLEDGMENTS

This work has received funding from Research Foundation−Flanders (FWO SB/1S30116N, FWO G086114, FWO G084818N) and the European Union's Horizon 2020 research and innovation program under the Marie Skłodowska-Curie grant agreement No. 675412 (H2020-MSCA-ITN-ND4ID).

REFERENCES

1. Berg J, Tymoczko J, Stryer L. 2007. Biochemistry. New York
2. Gesteland RF, Atkins JF. 1993. The RNA world: the nature of modern RNA suggests a prebiotic RNA world. New York
3. Wilson DS, Szostak JW. 1999. In Vitro Selection of Functional Nucleic Acids. Annu Rev Biochem. 68:611–647. doi: 10.1146/annurev.biochem.68.1.611
4. Walter NG, Engelke DR. 2002. Ribozymes: Catalytic RNAs that cut things, make things, and do odd and useful jobs. Biologist 49:199–203
5. Mitsuyasu RT, Merigan TC, Carr A, Zack JA, Winters MA, Workman C, Bloch M, Lalezari J, Becker S, Thornton L, Akil B, Khanlou H, Finlayson R, McFarlane R, Smith DE, Garsia R, Ma D, Law M, Murray JM, von Kalle C, Ely JA, Patino SM, Knop AE, Wong P, Todd A V, Haughton M, Fuery C, Macpherson JL, Symonds GP, Evans LA, Pond SM, Cooper DA. 2009. Phase 2 gene therapy trial of an anti-HIV ribozyme in autologous CD34+ cells. Nat Med. 15:285–92. doi: 10.1038/nm.1932
6. Zhang Y, Wang J, Cheng H, Sun Y, Liu M, Wu Z, Pei R. 2017. Conditional control of suicide gene expression in tumor cells with theophylline-responsive ribozyme. Gene Ther. 24:84–91. doi: 10.1038/gt.2016.78
7. Breaker RR, Joyce GF. 2014. The Expanding View of RNA and DNA Function. Chem Biol. 21:1059–1065. doi: 10.3174/ajnr.A1256.Functional
8. Silverman SK. 2008. Nucleic Acid Enzymes (Ribozymes and Deoxyribozymes): In Vitro Selection and Application. In: Wiley Encyclopedia of Chemical Biology
9. Kasprowicz A, Stokowa-Sołtys K, Jeżowska-Bojczuk M, Wrzesiński J, Ciesiołka J. 2017. Characterization of Highly Efficient RNA-Cleaving DNAzymes that Function at Acidic pH with No Divalent Metal-Ion Cofactors. ChemistryOpen. 6:46–56. doi: 10.1002/open.201600141
10. Nakano S, Horita M, Kobayashi M, Sugimoto N. 2017. Catalytic Activities of Ribozymes and DNAzymes in Water and Mixed Aqueous Media. Catalysts. 7:355. doi: 10.3390/catal7120355
11. Nesbitt SM, Erlacher HA, Fedor MJ. 1999. The internal equilibrium of the hairpin ribozyme: Temperature, ion and pH effects. J Mol Biol. 286:1009–1024. doi: 10.1006/jmbi.1999.2543
12. Perrotta AT, Been MD. 2006. HDV ribozyme activity in monovalent cations. Biochemistry. 45:11357–11365. doi: 10.1021/bi061215+
13. Saran R, Liu J. 2016. A Silver DNAzyme. Anal Chem. 88:4014–4020. doi: 10.1021/acs.analchem.6b00327
14. Nagraj N, Liu J, Sterling S, Wu J, Lu Y. 2009. DNAzyme catalytic beacon sensors that resist temperature-dependent variations. Chem Commun. 4103. doi: 10.1039/b903059j
15. Kosman J, Juskowiak B. 2011. Peroxidase-mimicking DNAzymes for biosensing applications: A review. Anal. Chim. Acta 707:7–17
16. Boersma AJ, Feringa BL, Roelfes G. 2009. Enantioselective Friedel–Crafts Reactions in Water Using a DNA-Based Catalyst. Angew Chemie Int Ed. 48:3346–3348. doi: 10.1002/anie.200900371
17. Li Y, Sen D. 1996. A catalytic DNA for porphyrin metallation. Nat Struct Biol. 3:743–747. doi: 10.1038/nsb0996-743
18. Santoro SW, Joyce GF. 1997. A general purpose RNA-cleaving DNA enzyme. Proc Natl Acad Sci. 94:4262–4266. doi: 10.1073/pnas.94.9.4262
19. Zhou W, Saran R, Liu J. 2017. Metal Sensing by DNA. Chem Rev. 117:8272–8325. doi: 10.1021/acs.chemrev.7b00063
20. Kim SU, Batule BS, Mun H, Shim W-B, Kim M-G. 2018. Ultrasensitive colorimetric detection of Salmonella enterica Typhimurium on lettuce leaves by HRPzyme-Integrated polymerase chain reaction. FOOD Control. 84:522–528. doi: 10.1016/j.foodcont.2017.09.010
21. Park Y, Lee CY, Kang S, Kim H, Park KS, Park HG. 2018. Universal, colorimetric microRNA detection strategy based on target-catalyzed toehold-mediated strand displacement reaction. Nanotechnology. 29:085501. doi:

10.1088/1361-6528/aaa3a3
22. Chen F, Bai M, Cao K, Zhao Y, Cao X, Wei J, Wu N, Li J, Wang L, Fan C, Zhao Y. 2017. Programming Enzyme-Initiated Autonomous DNAzyme Nanodevices in Living Cells. ACS Nano. 11:11908–11914. doi: 10.1021/acsnano.7b06728
23. Chen J, Zuehlke A, Deng B, Peng H, Hou X, Zhang H. 2017. A Target-Triggered DNAzyme Motor Enabling Homogeneous, Amplified Detection of Proteins. Anal Chem. 89:12888–12895. doi: 10.1021/acs.analchem.7b03529
24. Yang J, Tang M, Diao W, Cheng W, Zhang Y, Yan Y. 2016. Electrochemical strategy for ultrasensitive detection of microRNA based on MNAzyme-mediated rolling circle amplification on a gold electrode. Microchim ACTA. 183:3061–3067. doi: 10.1007/s00604-016-1958-5
25. Tabrizi SN, Tan LY, Walker S, Poljak M, Twin J, Garland SM, Bradshaw CS, Fairley CK, Mokany E, Poljak M, Bradshaw CS, Fairley CK, Bissessor M, Mokany E, Todd A V., Garland SM. 2016. Multiplex assay for simultaneous detection of mycoplasma genitalium and macrolide resistance using plexzyme and plexprime technology. PLoS One. 11:e0156740. doi: 10.1136/sextrans-2015-052270.106
26. Zhang P, He Z, Wang C, Chen J, Zhao J, Zhu X, Li C-Z, Min Q, Zhu J-J. 2015. In Situ Amplification of Intracellular MicroRNA with MNAzyme Nanodevices for Multiplexed Imaging, Logic Operation, and Controlled Drug Release. ACS Nano. 9:789–798. doi: 10.1021/nn506309d
27. Li X, Cheng W, Li D, Wu J, Ding X, Cheng Q, Ding S. 2016. A novel surface plasmon resonance biosensor for enzyme-free and highly sensitive detection of microRNA based on multi component nucleic acid enzyme (MNAzyme)-mediated catalyzed hairpin assembly. Biosens Bioelectron. 80:98–104. doi: 10.1016/j.bios.2016.01.048
28. Mokany E, Bone SM, Young PE, Doan TB, Todd A V. 2010. MNAzymes, a versatile new class of nucleic acid enzymes that can function as biosensors and molecular switches. J Am Chem Soc. 132:1051–1059. doi: 10.1021/ja9076777
29. Deborggraeve S, Dai JY, Xiao Y, Soh HT. 2013. Controlling the function of DNA nanostructures with specific trigger sequences. Chem Commun. 49:397–399. doi: 10.1039/C2CC36878A
30. Torabi S-F, Wu P, McGhee CE, Chen L, Hwang K, Zheng N, Cheng J, Lu Y. 2015. In vitro selection of a sodium-specific DNAzyme and its application in intracellular sensing. Proc Natl Acad Sci. 112:5903–5908. doi: 10.1073/pnas.1420361112
31. Mazumdar D, Nagraj N, Kim HK, Meng X, Brown AK, Sun Q, Li W, Lu Y. 2009. Activity, folding and Z-DNA formation of the 8-17 DNAzyme in the presence of monovalent ions. J Am Chem Soc. 131:5506–5515. doi: 10.1021/ja8082939
32. Zhou W, Zhang Y, Ding J, Liu J. 2016. In Vitro Selection in Serum: RNA-Cleaving DNAzymes for Measuring Ca2+and Mg2+. ACS Sensors. 1:600–606. doi: 10.1021/acssensors.5b00306
33. Saran R, Liu J. 2016. A comparison of two classic Pb2+-dependent RNA-cleaving DNAzymes. Inorg Chem Front. 3:494–501. doi: 10.1039/C5QI00125K
34. Li J, Lu Y. 2000. A Highly Sensitive and Selective Catalytic DNA Biosensor for Lead Ions. J Am Chem Soc. 122:10466–10467. doi: 10.1021/ja0021316
35. Ren K, Wu J, Ju H, Yan F. 2015. Target-driven triple-binder assembly of MNAzyme for amplified electrochemical immunosensing of protein biomarker. Anal Chem. 87:1694–1700. doi: 10.1021/ac504277z
36. Schubert S, Gül DC, Grunert HP, Zeichhardt H, Erdmann VA, Kurreck J. 2003. RNA cleaving “10-23” DNAzymes with enhanced stability and activity. Nucleic Acids Res. 31:5982–5992. doi: 10.1093/nar/gkg791
37. Gao J, Shimada N, Maruyama A. 2015. Enhancement of deoxyribozyme activity by cationic copolymers. Biomater Sci. 3:308–316. doi: 10.1039/C4BM00256C
38. Gao J, Shimada N, Maruyama A. 2015. MNAzyme-catalyzed nucleic acid detection enhanced by a cationic copolymer. Biomater Sci. 3:716–720. doi: 10.1039/C4BM00449C
39. Levy M, Ellington AD. 2003. Exponential growth by cross-catalytic cleavage of deoxyribozymogens. Proc Natl Acad Sci U S A. 100:6416–21. doi: 10.1073/pnas.1130145100
40. Gerasimova Y V., Cornett EM, Edwards E, Su X, Rohde KH, Kolpashchikov DM. 2013. Deoxyribozyme cascade for visual detection of bacterial RNA. ChemBioChem. 14:2087–2090. doi: 10.1002/cbic.201300471
41. Bone SM, Hasick NJ, Lima NE, Erskine SM, Mokany E, Todd A V. 2014. DNA-only Cascade: A universal tool for signal amplification, enhancing the detection of target analytes. Anal Chem. 86:9106–9113. doi: 10.1021/ac501811r
42. So PTC, Dong CY. 2002. Fluorescence Spectrophotometry. Encycl Life Sci. 1–4. doi: 10.1038/npg.els.0002978
43. Tomin VI. 2008. Effect of temperature on the dynamic quenching of the dual fluorescence of molecules. Opt Spectrosc. 104:838–845. doi: 10.1134/S0030400X08060064
44. Gao Z, Hou L, Xu M, Tang D. 2015. Enhanced Colorimetric Immunoassay Accompanying with Enzyme Cascade Amplification Strategy for Ultrasensitive Detection of Low-Abundance Protein. Sci Rep. 4:1–8. doi: 10.1038/srep03966